Journal of Applied Polymer Science

Effects of plasticization and hydrostatic pressure on tensile properties of PMMA under compressed carbon dioxide and nitrogen

Tomoaki Taguchi, Hiromu Saito
Department of Organic and Polymer Materials Chemistry, Tokyo University of Agriculture and Technology, Koganei-Shi, Tokyo 184-8588, Japan
Correspondence to: H. Saito (E-mail: hsaitou@cc.tuat.ac.jp)

ABSTRACT: We investigated the stress−strain behavior of PMMA films under compressed CO_2 and N_2. The elongation at break increased and the stress decreased with increasing CO_2 pressure at pressures above 3 MPa, indicating that the tensile property changed from brittle to ductile under compressed CO_2. In contrast, the material property became more brittle under compressed CO_2 at pressures below 2 MPa and under compressed N_2. By depressurizing the compressed gas and excluding the hydrostatic pressure, the property of the gas-absorbed specimen changed from brittle to ductile. These results suggest that deformability by molecular orientation is enhanced by the plasticizing effect caused by a large amount of absorbed gas while it is suppressed by the effect of hydrostatic pressure caused by a small amount of absorbed gas. Conversely, the elastic modulus decreased under both compressed CO_2 and N_2, but the decrease under CO_2 was much larger than that under N_2, suggesting that distortion in the elastic region is dominated by the plasticization effect. © 2016 Wiley Periodicals, Inc. J. Appl. Polym. Sci. **2016**, *133*, 43431.

KEYWORDS: absorption; carbon dioxide; mechanical properties; nitrogen; PMMA

Received 16 November 2015; accepted 10 January 2016
DOI: 10.1002/app.43431

INTRODUCTION

Polymer films are often used under compressed gas for various materials: e.g., gas separation membranes,[1–4] gas barrier materials for food packaging, medicine packaging, hoses, and tire tubes.[5–7] Under compressed gas, polymer films are usually deformed by a decrease of the elastic modulus or fractured by a reduction of the deformability. Such physical changes are not preferable for use under compressed gas. Therefore, it is important to know the changes in the tensile properties under compressed gas. However, there are few studies that focus on the tensile properties of polymers under compressed gas.[8–12]

It is thought that compressed gas causes two competing effects on polymer films. One is the plasticization effect caused by the absorption of gas into polymers.[13–21] The gas is absorbed into the free volume between polymer chains, so that chain mobility is accelerated,[22–26] dilation occurs,[27] deformation is enhanced,[8–12] the glass transition temperature is depressed,[21,28–32] and viscosity decreases[21,33–36] with an increase in the absorbed gas in the polymers associated with the increased gas pressure. Another effect is that of hydrostatic pressure, which is the resistance to deformation caused by the vitrification resulting from the reduction of free volume. The effect of hydrostatic pressure is usually estimated by the tensile properties under compressed oil, and it was reported that elastic modulus and yield stress increase while the elongation at break decreases with increasing pressure.[37–43] A reduction of gas permeation was suggested to be caused by hydrostatic pressure.[44] Dielectric measurement revealed that molecular motion is suppressed by increasing hydrostatic pressure.[45] However, since the plasticizing effect and hydrostatic pressure effect are discussed separately, the two competing effects on tensile properties have not been clarified, although they are important for understanding the use of polymer films under compressed gas.

In this article, to more thoroughly understand the two competing effects of plasticization and hydrostatic pressure on tensile properties under compressed gas, we investigated the stress−strain behavior of noncrystalline glassy poly(methyl methacrylate) (PMMA) under compressed gas at various pressures by using a specially designed tensile-deformation instrument for measurements under compressed gas. CO_2 and N_2 were used as the compressed gases because the solubility of CO_2 is large while that of N_2 is small.[19,24,46–48] The solubility constants of CO_2 and N_2 in PMMA are 0.26 cm^2(STP)/g atm and 0.045 cm^2(STP)/g atm, respectively.[47] The large solubility of CO_2 is attributed to a dipole-dipole interaction between CO_2 and the carbonyl function group of PMMA[19,49] due to its Lewis acid–base nature.[50] Therefore, it is considered that the plasticizing effect is larger under the compressed CO_2 than that under the compressed N_2, so that the

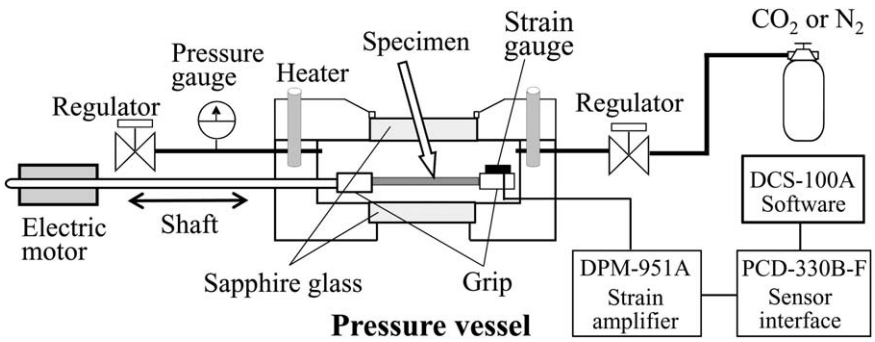

Figure 1. Schematic illustration of a stretching instrument for tensile-deformation measurements under compressed gas.

two competing effects of plasticization and hydrostatic pressure can be compared by using CO_2 and N_2. To exclude the hydrostatic pressure effect and identify the plasticizing effect, we also carried out tensile-deformation measurement for the gas-absorbed-depressurized specimen. The deformability and modulus under the compressed gas are discussed in terms of two molecular mechanisms on deformation, i.e., molecular orientation and distortion.

EXPERIMENTAL

Materials

The PMMA specimen used in this study was a commercial product (Acrypet MD001, $M_w = 11.0 \times 10^4$ g/mol, $M_n = 5.0 \times 10^4$ g/mol, $M_w/M_n = 2.2$) supplied by Mitsubishi Rayon Co., Ltd. The PMMA pellet was compression molded between metal plates at 220 °C for 5 min to obtain a film specimen with a thickness of about 200 μm and then cooled at room temperature.

Tensile Measurement for Compressed Gas

To perform *in situ* tensile deformation measurements of the specimens under compressed gas, we designed a stretching instrument with a stainless steel pressure vessel, as shown in Figure 1. Two sapphire glass windows were mounted on the pressure vessel to enable observation. The crosshead of the elongation instrument traveled up to a strain limit of 2.8 at a speed of 5 mm/min in the pressure vessel (Taiatsu Techno Corporation). Movement of the crosshead was regulated by a shaft connected to a linear motor (Oriental Motor Co., Ltd.) outside the vessel. The shaft was passed through a special rubber gasket from Chemraz (Greene Tweed Co., Ltd.) to prevent leakage of the inert gas. A strain gauge (KFR-2-120-C1-16 Kyowa Electronic Instruments Co., Ltd.) was attached at the surface of the crosshead to measure stress during the stretching of the polymer film. Specifically, the strain gauge was deformed by the stress applied to the polymer film and the voltage was caused by a change in the electrical resistance in the strain gauge. The voltage was amplified by DM-951 amplifier (Kyowa Electronic Instruments Co., Ltd.) and the analog voltage was converted into digital data by a PCD-330B-F sensor interface (Kyowa Electronic Instruments Co., Ltd.). The digital data was recorded and the applied stress was calculated with DCS-100A software (Kyowa Electronic Instruments Co., Ltd.).

A dumbbell-shaped film specimen was cut from the PMMA film and was mounted on the stretching instrument. After sealing, compressed CO_2 or N_2 was injected into the pressure vessel with a syringe pump (NPKX-500, Nihon Seimitsu Kagaku Co., Ltd.) at room temperature and was kept there for 1 h to dissolve the compressed gas in the specimen. Then, the specimen was stretched under the compressed gas. Note here that the tensile property was not changed by absorbing CO_2 or N_2 for a time longer than 1 h, so that 1 h is sufficient for absorbing the compressed gas in the specimens. The pressure of CO_2 or N_2 within the vessel was monitored with an output pressure transducer and was kept constant with a back-pressure regulator (TESCOM 26-1763-24). The temperature was set at 30 °C during this study by an Autotune temperature controller unit with a thermocouple. The tensile deformation measurements were carried out above twice at same pressure to confirm the reliability of the data.

To investigate the stress−strain behavior of the gas-absorbed specimen under the absence of hydrostatic pressure, the compressed gas was absorbed into the film specimen mounted on the stretching instrument for 1 h at 30 °C. Then, the tensile-deformation measurement was carried out immediately under air at ambient pressure after the gas was released from the pressure vessel, i.e., the tensile-deformation measurement was carried out for the gas-absorbed depressurized specimen.

RESULTS AND DISCUSSION

Figures 2 and 3 show the stress−strain curves of the PMMA films under compressed CO_2 and N_2, respectively, at various pressures obtained by the *in situ* tensile measurements up to a strain limit of 2.8. The stress−strain curve under air at ambient pressure of 0.1 MPa is also shown for the property in the absence of the plasticizing effect. Under air at ambient pressure, the specimen was fractured at a small strain, i.e., elongation at break was only 0.09. This is characteristic of brittle behavior. On the other hand, the yield point appeared at around a strain of 0.1 and the plateau region was observed at a strain above 0.3 under CO_2 (Figure 2). Thus, elongation at break became longer under compressed CO_2 than that under air at ambient pressure. Such deformability is characteristic of ductile behavior. With increased CO_2 pressure, elongation at break increased, and became longer than a strain limit of 2.8 when the CO_2 pressure was above 5 MPa. By association with the increased elongation at break, the yield stress and the stress at the plateau region

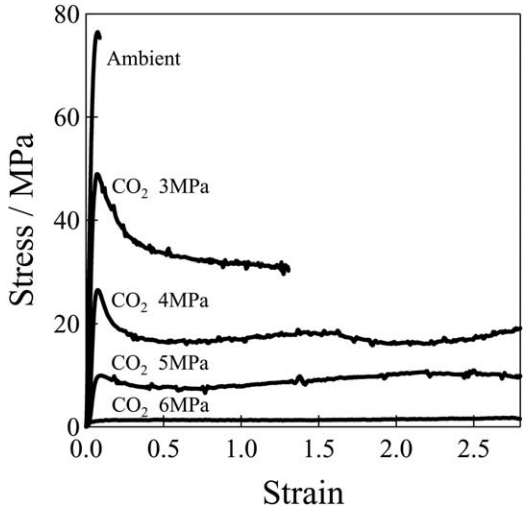

Figure 2. Stress–strain curve of PMMA under CO_2 at various pressures.

decreased sharply with increased CO_2 pressure. These results indicate that the property changes from brittle to ductile by absorbing CO_2 and that the deformability increases with increased CO_2 pressure by association with the increased amount of CO_2 absorbed in the PMMA. The decrease of the stress in the noncrystalline glassy polymer of PMMA under compressed CO_2 was much larger than those observed in crystalline polymers such as poly(ethylene terephthalate) (PET),[8,9] nylon,[10] ultrahigh molecular weight polyethylene,[11] and polypropylene.[12] The difference of the plasticization effect might be attributed to the small amount of the absorbed CO_2 in crystalline polymers due to the existence of the crystalline region in which the gas is insoluble.[51] Owing to the small amount of the absorbed CO_2, the hydrostatic pressure effect was observed in PET at high CO_2 pressure; i.e., the stress increased with CO_2 pressure at the pressure above 7 MPa.[8,9]

In contrast, elongation at break became shorter under compressed N_2 than that under air at ambient pressure and the specimen was fractured before the yield point, i.e., it was 0.07 and 0.09 under N_2 at 5 MPa and under air at ambient pressure, respectively (Figure 3). With increased N_2 pressure, elongation at break decreased. These results indicate that the material property becomes more brittle under the compressed N_2 and the deformability decreases with increased N_2 pressure.

Thus, the tensile properties observed under the compressed CO_2 and N_2 were opposite. Specifically, the property became ductile under compressed CO_2 while it became more brittle under compressed N_2. It is considered that the compressed gas causes two competing effects on polymer films: one is a plasticizing effect and the other is a hydrostatic pressure effect. The opposite tensile properties observed under compressed CO_2 and N_2 are attributed to the different contributions of the two competing effects of plasticization and hydrostatic pressure on PMMA film under compressed CO_2 and N_2. The plasticizing effect is large when the amount of the absorbed gas is large and the amount of CO_2 absorbed in PMMA is large while that of N_2 is small[19,24,46–48]; i.e., the solubility constants of CO_2 and N_2 in PMMA are 0.26 cm^2(STP)/g atm and 0.045 cm^2 (STP)/g atm, respectively.[47] On the other hand, the elongation at break decreases with increasing pressure by the hydrostatic pressure effect.[36–43] Thus, the results shown in Figures 2 and 3 suggest that the plasticization effect is large under compressed CO_2 while the hydrostatic pressure effect is large under compressed N_2. Owing to the plasticization effect under compressed CO_2, the plasticized PMMA is easily oriented with less force due to the acceleration of the molecular motion,[8–26] so that the property becomes ductile. On the other hand, since the amount of absorbed gas is small under compressed N_2, the hydrostatic pressure effect dominates. Because of the hydrostatic effect under compressed N_2, the deformation is suppressed due to the reduction in free volume,[34–40] so that the property becomes more brittle.

As shown in Figure 4, elongation at break was shorter at a low pressure below 2 MPa under compressed CO_2 than that under air at ambient pressure, although it was longer at a higher pressure above 3 MPa, as shown in Figure 2. That is, the property becomes more brittle under CO_2 at low pressure in which the

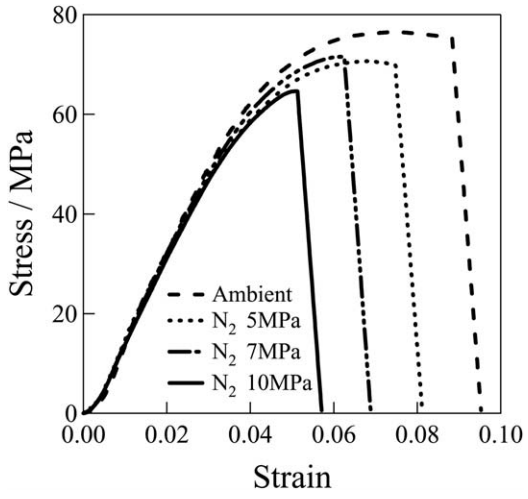

Figure 3. Stress–strain curve of PMMA under N_2 at various pressures.

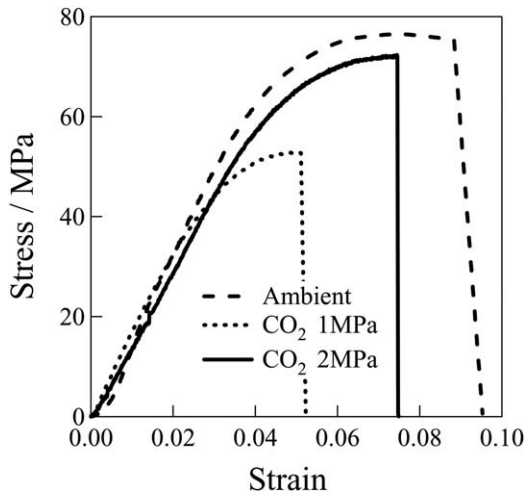

Figure 4. Stress–strain curve of PMMA at low pressure below 2 MPa under CO_2.

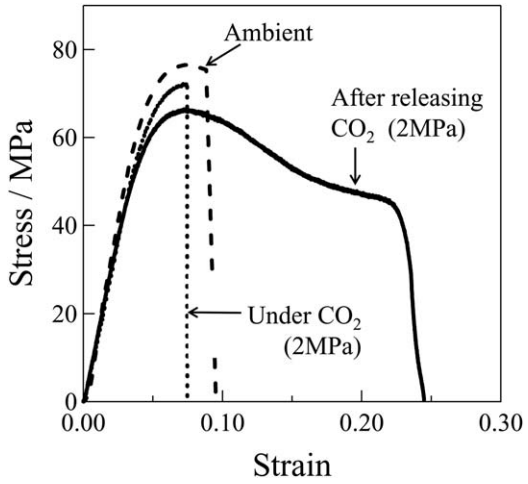

Figure 5. Stress–strain curve of PMMA under CO_2 of 2 MPa and CO_2-absorved PMMA under air at ambient pressure after releasing CO_2 of 2 MPa.

amount of absorbed CO_2 is small. This behavior is similar to that observed under compressed N_2 in which the hydrostatic pressure effect is seen due to small amount of absorbed gas. The result supports the above scenario that deformation is suppressed by the hydrostatic pressure effect when the amount of absorbed gas is small.

In order to exclude the hydrostatic pressure effect, the stress−strain behavior of CO_2-absorbed PMMA was measured under air at ambient pressure after releasing CO_2 of 2 MPa. Figure 5 shows the stress−strain curve of the CO_2-absorbed depressurized PMMA in the absence of hydrostatic pressure. For comparison, the stress−strain curves of PMMA under CO_2 at 2 MPa and under air at ambient pressure are also shown in Figure 5. The CO_2-absorbed depressurized PMMA exhibited ductile behavior, i.e., the strength was lower and the elongation at break was much longer in the absence of hydrostatic pressure than were those under compressed CO_2 at pressures below 2 MPa and under air at ambient pressure. These results suggest that the

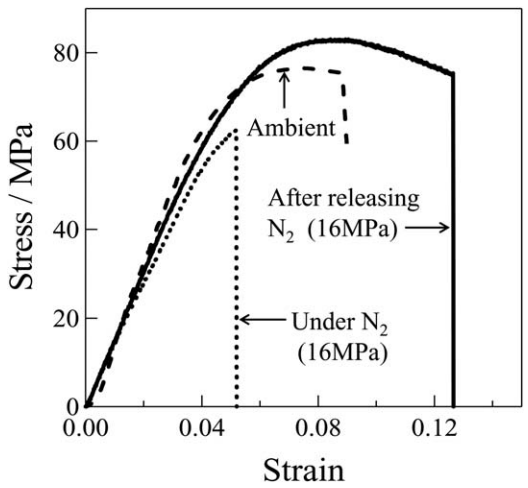

Figure 6. Stress–strain curve of PMMA under N_2 of 16 MPa and N_2-absorbed PMMA under air at ambient pressure after releasing N_2 of 16 MPa.

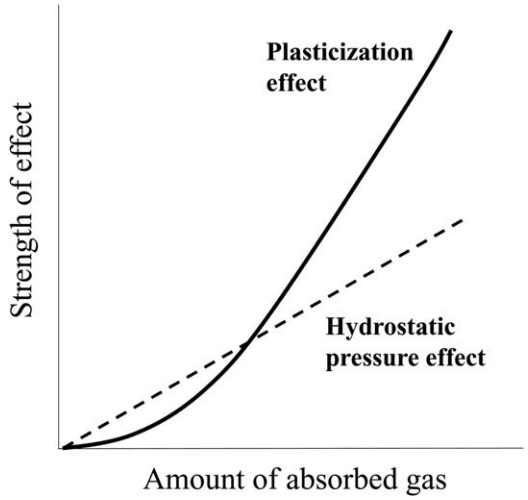

Figure 7. Schematic illustration of the strength of the plasticized effect and the hydrostatic pressure effect with the amount the absorbed gas in PMMA.

property becomes ductile by plasticization due to absorbed CO_2 in the absence of hydrostatic pressure, although it becomes brittle in the presence of hydrostatic pressure under compressed CO_2 at pressures below 2 MPa. Thus, the decrease of deformability under CO_2 at low pressure below 2 MPa, shown in Figure 4, suggests that the hydrostatic pressure effect dominates when the amount of absorbed gas is small under compressed CO_2.

As shown in Figure 6, the N_2-absorbed depressurized PMMA also exhibited increases of deformability in the absence of hydrostatic pressure, although the deformability decreased under compressed N_2 (Figure 3). Elongation at break became longer from 0.05 to 0.13 by releasing N_2 of 16 MPa. The results suggest that the property becomes ductile by plasticization due to absorbed N_2 in the absence of hydrostatic pressure, although it becomes more brittle in the presence of hydrostatic pressure. These results confirm that deformation is enhanced by the plasticizing effect while it is suppressed by the hydrostatic pressure effect.

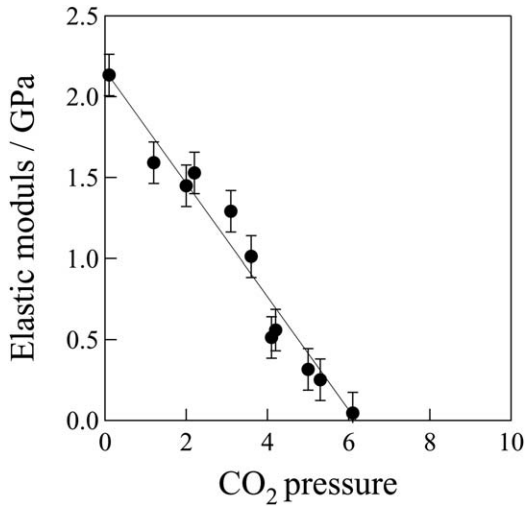

Figure 8. Elastic modulus of PMMA under CO_2 at various pressures.

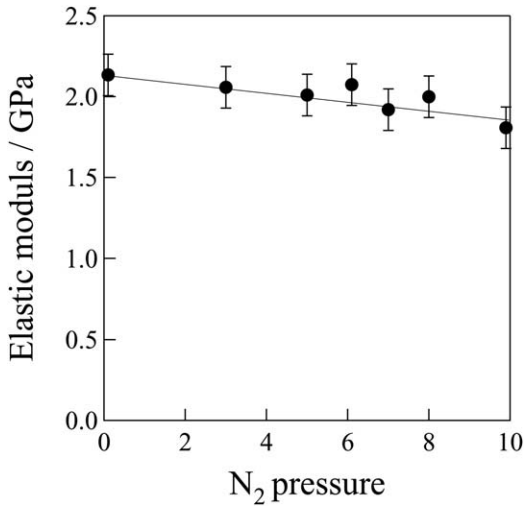

Figure 9. Elastic modulus of PMMA under N_2 at various pressures.

Thus, the two competing effects contribute to the tensile property of PMMA. The hydrostatic pressure effect dominates when the amount of gas is small while the plasticizing effect dominates when the amount of gas is large under compressed gas, as schematically shown in Figure 7.

Figures 8 and 9 show the elastic modulus of the PMMA films at various pressures under CO_2 and N_2 obtained from the initial slopes of Figures 2 and 3, respectively. Under air at ambient pressure, the elastic modulus was approximately 2.2 GPa. The elastic modulus decreased sharply with increased pressure under compressed CO_2; it became approximately 0 at around a pressure of 6 MPa when the glass transition temperature became lower than the measurement temperature (30 °C) by the depression of the glass transition temperature[21,28–32] (Figure 8). The decrease of the elastic modulus is attributed to the plasticization effect by the compressed CO_2. The plasticization effect becomes larger as the amount of absorbed CO_2 increases with increased CO_2 pressure.

Although deformability decreases by the hydrostatic pressure effect under compressed N_2, the elastic modulus did not increase but decreased slightly with increased N_2 pressure. E.g., it was approximately 2.2 and 1.8 under air at ambient pressure and under N_2 of 10 MPa, respectively (Figure 9). This result suggests that the plasticizing effect dominates the elastic modulus under compressed N_2. That is, the elastic modulus decreased as the amount of absorbed N_2 was larger with increased N_2 pressure. The decrease in the elastic modulus under compressed N_2 was much smaller than that under compressed CO_2, indicating that the plasticizing effect on the elastic modulus is much smaller under compressed N_2 compared with that under compressed CO_2 due to the small amount of absorbed N_2. In other words, the amount of absorbed N_2 is much smaller than that of absorbed CO_2.[19,24,46–48]

The interesting result here is that the plasticization effect was seen in the elastic modulus while the hydrostatic pressure effect was seen in the deformability under compressed N_2. The difference might be attributed to the different contributions of the plasticization effect and the hydrostatic pressure effect on the

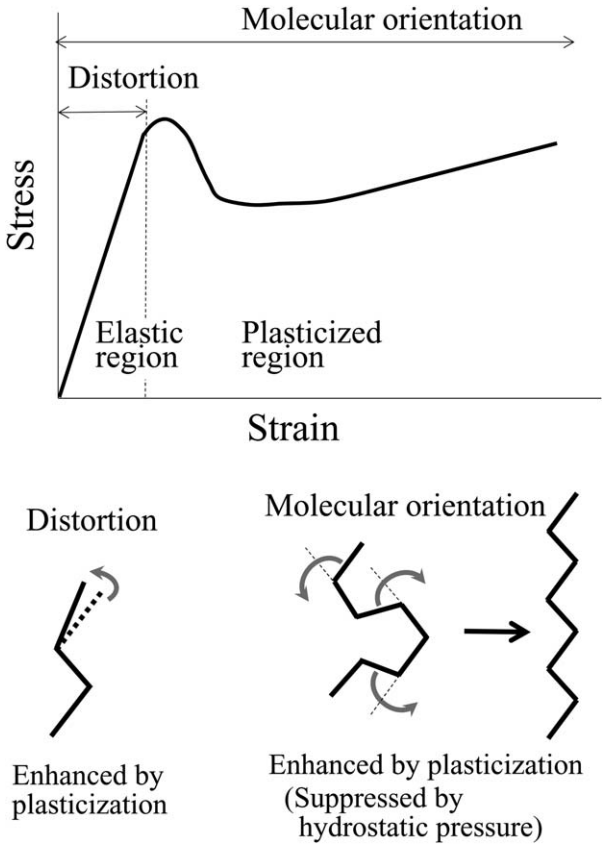

Figure 10. Schematic illustration of distortion and molecular orientation.

two molecular mechanisms of deformation, distortion and molecular orientation,[52–56] as shown in the illustration of Figure 10. The distortion is local change of the intersegment distance by torsion around the main-chain bonds or local displacement of the interchain spacing. On the other hand, the molecular orientation is relatively long-range conformational rearrangements by orientation of the main-chain segments. The deformation in the elastic region is attributed to both distortion and molecular orientation, while that in the plasticized region is attributed only to molecular orientation. The modulus by distortion is two decades higher than that by molecular orientation, so that the modulus in the elastic region is mainly attributed to distortion.[56] Because only the plasticization effect was observed in the elastic modulus, distortion is dominated by the plasticization effect. On the other hand, since the plasticization effect was observed under compressed CO_2 at high pressure while the hydrostatic pressure effect was observed under compressed CO_2 at low pressure and under compressed N_2, the molecular orientation is enhanced by the plasticization effect when the amount of absorbed gas is large while it is suppressed by the hydrostatic pressure effect when the amount of absorbed gas is small.

CONCLUSIONS

The two competing effects of plasticization and hydrostatic pressure on the tensile properties of PMMA were clarified by comparing stress−strain behavior under compressed CO_2 and N_2. The property changed from brittle to ductile with increased

pressure under CO_2 at high pressure associated with increasing the amount of absorbed CO_2, while it became more brittle under CO_2 at low pressure and under N_2. Although the property was brittle under the compressed gas, it changed to ductile by depressurization and stretching in the absence of hydrostatic pressure. These results suggest that the plasticizing effect dominates the molecular orientation and enhances deformation when the amount of absorbed gas is large, while the hydrostatic pressure effect dominates and suppresses deformation when the amount of absorbed gas is small. On the other hand, the elastic modulus decreased with increased pressure under both compressed CO_2 and N_2, suggesting that the distortion in the elastic region is dominated by the plasticizing effect. Quantitative analysis of the elastic modulus reveals that the modulus depending on the CO_2 pressure is correlated to the molecular motion depending on the temperature. The quantitative results for elastic modulus will be reported in the near future.

ACKNOWLEDGMENTS

This work was partially supported by the Japan Society for the Promotion of Science (Grant-in-Aid for Scientific Research (C), No. 15K05620).

REFERENCES

1. Freeman, B.; Yampolskii, Y., Eds. Membrane of Gas Separation; Wiley: New York, **2010**.
2. Yampolskii, Y. *Macromolecules* **2012**, *45*, 3298.
3. Sanders, D. F.; Smith, Z. P.; Guo, R.; Robeson, L. M.; McGrath, J. E.; Paul, D. R.; Freeman, B. D. *Polymer* **2013**, *54*, 4729.
4. Adewole, J. K.; Ahmad, A. L.; Ismail, S.; Leo, C. P. *Int. J. Greenhouse Gas Control* **2013**, *17*, 46.
5. Boyer, S. A. E.; Klopffer, M. H.; Martin, J.; Grolier, J. P. E. *J. Appl. Polym. Sci.* **2007**, *103*, 1706.
6. Hatzigrigoriou, N. B.; Papaspyrides, C. D. *J. Appl. Polym. Sci.* **2011**, *122*, 3719.
7. Siracusa, V. *Int. J. Polym. Sci.* **2012**, *2012*, Article ID 302029.
8. Hobbs, T.; Lesser, A. J. *J. Polym. Sci. Part B: Polym. Phys.* **1999**, *37*, 1881.
9. Hobbs, T.; Lesser, A. J. *Polymer* **2000**, *41*, 6223.
10. Hobbs, T.; Lesser, A. J. *Polym. Eng. Sci.* **2001**, *41*, 135.
11. Garcia-Leiner, M.; Song, J.; Lesser, A. J. *J. Polym. Sci. Part B: Polym. Phys.* **2003**, *41*, 1375.
12. Osaka, N.; Kono, F.; Saito, H. *J. Appl. Polym. Sci.* **2013**, *127*, 1228.
13. Shieh, Y. T.; Su, J. H.; Manivannan, G.; Lee, P. H. C.; Sawan, S. P.; Spall, W. D. *J. Appl. Polym. Sci* **1996**, *59*, 707.
14. Kazarian, S. G. *Polym. Sci. Ser. C* **2000**, *42*, 78.
15. Hilic, S.; Boyer, S. A. E.; Pádua, A. A. H.; Grolier, J. P. E. *J. Polym. Sci. Part B: Polym. Phys.* **2001**, *39*, 2063.
16. Prabhakar, R. S.; De Angelis, M. G.; Sarti, G. C.; Freeman, B. D.; Coughlin, M. C. *Macromolecules* **2005**, *38*, 7043.
17. Fleming, O. S.; Andrew Chan, K. L.; Kazarian, S. G. *Polymer* **2006**, 464649.
18. Visser, T.; Wessling, M. *Macromolecules* **2007**, *40*, 4992.
19. Eslami, H.; Kesik, M.; Karimi-Varzaneh, H. A.; Müller-Plathe, F. *J. Chem. Phys.* **2013**, *139*, 1249021.
20. Kawate, K.; Osaka, N.; Saito, H. *Polymer* **2013**, *54*, 2406.
21. Gutiérrez, C.; Rodríguez, J. F.; Gracia, I.; de Lucas, A.; García, M. T. *J. Appl. Polym. Sci.* **2015**, *132*, 41696.
22. Kamiya, Y.; Mizoguchi, K.; Naito, Y. *J. Polym. Sci. Part B: Polym. Phys.* **1990**, *28*, 1955.
23. Goel, S. K.; Beckman, E. J. *Polymer* **1993**, *34*, 1410.
24. Hirota, S.; Tominaga, Y.; Asai, S.; Sumita, M. *J. Polym. Sci. Part B: Polym. Phys.* **2005**, *43*, 2951.
25. Matsumiya, Y.; Inoue, T.; Iwashige, T.; Watanabe, H. *Macromolecules* **2009**, *42*, 4712.
26. Neyertz, S.; Brown, D. *Macromolecules* **2013**, *46*, 2433.
27. Kamiya, Y.; Mizoguchi, K.; Terada, K.; Fujiwara, Y.; Wang, J. S. *Macromolecules* **1998**, *31*, 472.
28. Chiou, J. S.; Barlow, J. W.; Paul, D. R. *J. Appl. Polym. Sci.* **1985**, *30*, 2633.
29. Zhang, Z.; Handa, Y. P. *J. Polym. Sci. Part B: Polym. Phys.* **1998**, *36*, 977.
30. Edwards, R. R.; Tao, Y.; Xu, S.; Wells, P. S.; Yun, K. S.; Parcher, J. F. *J. Polym. Sci. Part B: Polym. Phys.* **1998**, *36*, 2537.
31. Cao, G. P.; Liu, T.; Roberts, G. W. *J. Appl. Polym. Sci.* **2010**, *115*, 2136.
32. Tsioptsias, C.; Panayiotou, C. *Thermochim. Acta* **2011**, *521*, 98.
33. Kwag, C.; Manke, C. W.; Gulari, E. *J. Polym. Sci. Part B: Polym. Phys.* **1999**, *37*, 2771.
34. Royer, J. R.; Gay, Y. J.; Desimone, J. M.; Khan, S. A. *J. Polym. Sci. Part B: Polym. Phys.* **2000**, *38*, 3168.
35. Areerat, S.; Nagata, T.; Ohshima, M. *Polym. Eng. Sci.* **2002**, *42*, 2234.
36. Kelly, C. A.; Howdle, S. M.; Shakesheff, K. M.; Jenkins, M. J.; Leeke, G. A. *J. Polym. Sci. Part B: Polym. Phys.* **2012**, *50*, 1383.
37. Laka, M. G.; Dzenis, A. A. *Mekhanika Polimerov* **1967**, *3*, 1043.
38. Rabinowitz, S.; Ward, I. M. *J. Mater. Sci.* **1970**, *5*, 29.
39. Christiansen, A. W.; Bear, E.; Radcliffe, S. V. *Phil. Mag.* **1971**, *24*, 451.
40. Parry, E. J.; Tabor, D. *J. Mater. Sci.* **1973**, *8*, 1510.
41. Silano, A. A.; Pae, K. D.; Sauer, J. A. *J. Appl. Phys.* **1977**, *48*, 4076.
42. Spitzig, W. A.; Richmond, O. *Polym. Eng. Sci.* **1979**, *19*, 1129.
43. Chakkarapani, V.; Ravi-Chandar, K.; Liechti, K. M. *J. Eng. Mater. Technol.* **2006**, *128*, 489.
44. Miranda, L. D.; Bell, R. J.; Short, R. T.; van Amerom, F. H. W.; Byrne, R. H. *J. Membr. Sci.* **2011**, *385386*, 49.
45. Roland, C. M.; Casalini, R. *Polymer* **2007**, *48*, 5747.
46. Duriff, P. L.; Griskey, R. G. *AIChE J* **1966**, *12*, 1147.
47. Paterson, R.; Yampol'skii, Y. *J. Phys. Chem. Ref. Data* **1999**, *28*, 1225.
48. Yamamoto, Y.; Maegawa, M.; Kumazawa, H. *J. Appl. Polym. Sci* **2003**, *87*, 1068.

49. Fried, J. R.; Li, W. *J. Appl. Polym. Sci.* **1990**, *41*, 1123.

50. Kazarian, S. G.; Vincent, M. F.; Bright, F. V.; Liotta, C. L.; Eckert, C. A. *J. Am. Chem. Soc.* **1996**, *118*, 1729.

51. Yamamura, Y.; Yoshida, K.; Kawate, K.; Osaka, N.; Saito, H. *Polym. J.* **2010**, *42*, 419.

52. Haward, R. N., Young, R. J. The Physics of Glassy Polymers, 2nd ed.; Springer: London, **1997**.

53. Yannas, I. V.; Luise, R. R. *J. Macromol. Sci. Phys.* **1982**, *B21*, 443.

54. Koenen, J. A.; Heise, B.; Kilian, H. G. *J. Polym. Sci. Part B: Polym. Phys.* **1989**, *27*, 1235.

55. Priss, L. S.; Vishnyakov, I. I.; Pavlova, I. P. *Int. J. Polym. Mater.* **1980**, *8*, 85.

56. Takahashi, S.; Saito, H. *Macromolecules* **2004**, *37*, 1062.